



Article

Laminaria hyperborea as a Source of Valuable Glyceroglycolipids—A Characterization of Galactosyldiacilglycerols in Stipe and Blade by HPLC-MS/MS

Lena Foseid , Hanne Devle , Carl Fredrik Naess-Andresen and Dag Ekeberg * 

Faculty of Chemistry, Biotechnology and Food Science, Norwegian University of Life Sciences, P.O. Box 5003, 1432 Ås, Norway

* Correspondence: dag.ekeberg@nmbu.no; Tel.: +47-6723-2464

Abstract: *Laminaria hyperborea* (Gunnerus) Foslie 1885 is a seaweed native to the North Atlantic, which is utilized in the production of alginate. Its potential as a source of bioactive lipids remains unexplored. In this study, mono- and digalactosyldiacylglycerols (MGDG and DGDG) were identified in stipe and blade from *L. hyperborea* for the first time. Samples were harvested off the west coast of Norway in May 2018. Lipids were extracted with chloroform:methanol (2:1, v/v) and fractionated using solid phase extraction, whereupon the fatty acid content was determined by gas chromatography-mass spectrometry. The fatty acid profile was used to predict the mass of the glyceroglycolipids. A total of 103 and 161 molecular species of MGDG, and 66 and 136 molecular species of DGDG were identified in blade and stipe, respectively, by HPLC-ESI-MS/MS. The most abundant molecular species were identified from the total ion chromatograms. According to these, MGDG(20:5/18:4, 18:4/18:4, 16:0/18:1, 14:0/18:2, 14:0/18:1) and DGDG(20:5/18:4, 16:0/18:1, 14:0/18:1) were the most abundant in blade. On the other hand, in stipe, the most abundant molecular species were MGDG (14:0/18:2, 14:0/18:1, 16:0/18:1) and DGDG (14:0/18:1). The purpose of this study is to highlight the potential application of *L. hyperborea* in a biotechnological context.

Keywords: glyceroglycolipids; monogalactosyldiacylglycerol; digalactosyldiacylglycerol; HPLC-MS/MS; GC-MS; seaweed



Citation: Foseid, L.; Devle, H.; Naess-Andresen, C.F.; Ekeberg, D. *Laminaria hyperborea* as a Source of Valuable Glyceroglycolipids—A Characterization of Galactosyldiacilglycerols in Stipe and Blade by HPLC-MS/MS. *AppliedChem* **2022**, *2*, 185–198. <https://doi.org/10.3390/appliedchem2040013>

Academic Editor: Jason Love

Received: 8 September 2022

Accepted: 23 September 2022

Published: 29 September 2022

Publisher's Note: MDPI stays neutral with regard to jurisdictional claims in published maps and institutional affiliations.



Copyright: © 2022 by the authors. Licensee MDPI, Basel, Switzerland. This article is an open access article distributed under the terms and conditions of the Creative Commons Attribution (CC BY) license (<https://creativecommons.org/licenses/by/4.0/>).

1. Introduction

Laminaria hyperborea, also known as tangleweed, cuvie, or simply kelp, is an edible seaweed common to the North Atlantic. Traditionally it has been used as both food and feed in the coastal areas of Northern Europe. Today, *L. hyperborea* is mainly harvested for alginate extraction. During this process, the stipe and blade of *L. hyperborea* is separated prior to utilization. In Europe, this commercial exploitation is centered in Norway, where the estimated biomass of *L. hyperborea* is 59 million tonnes [1]. Currently, less than 0.5% of this standing wild stock is harvested yearly [2]; thus, the potential for expanded utilization of this marine resource is tremendous. Additionally, from both economical and sustainable perspectives, further utilization of the leftover biomass from alginate production is desired.

Seaweed is recognized as a potential source of bioactive phytochemicals, among them, bioactive lipids. The bioactive and nutritional potential of the lipid fraction of *L. hyperborea* is largely unexplored. The most abundant lipids in seaweed are glyceroglycolipids, found mainly in the thylakoid and chloroplast membranes [3,4]. These glyceroglycolipids account for around 80% of the lipid content in thylakoids, with the remaining lipids being mostly phosphatidylglycerols and other glycerophospholipids [3]. The blade(s) of seaweed species have increased surface area to maximize the capacity for photosynthesis, and are therefore expected to have a higher content of thylakoid and chloroplast membranes compared to the stipe.

Glyceroglycolipids contain one or more monosaccharide moieties in the *sn*-3 position on a diacyl-glycerol. In plants, the most abundant groups of glyceroglycolipids are the monogalactosyldiacylglycerols (MGDG) and digalactosyldiacylglycerols (DGDG), containing one and two galactose moieties in the *sn*-3 position, respectively. Acyl chains are attached in the *sn*-1 and *sn*-2 positions.

The bioactivity of these lipids is dependent on both their carbohydrate moiety, acyl chain lengths, and degree of unsaturation [5]. MGDG and DGDG from seaweed have been shown to exhibit a range of bioactive properties, including anti-oxidant [6], anti-algal [7], anti-tumor/cancer [8–11], anti-inflammatory [5,9,12–16], anti-bacterial [17,18], anti-fungal [17,19], anti-viral [20], and herbivore-deterrent [21]. Promisingly, the use of MGDG as anti-inflammatory drugs has shown equal or better effects than the standard drugs in use, at non-cytotoxic concentrations [12,13,16]. In recent years, there has been a focus on in-depth studies of the lipidomes of seaweed and their bioactivity. The lipid profiles for several red [6,9,22,23], and a few green [24,25] and brown [26,27] seaweed have been reported (mainly by the same research group). Hydrophilic interaction liquid chromatography (HILIC)-tandem mass spectrometry (MS/MS) is the most common method of lipid analysis at the molecular level, and the number of identified molecular species range from 22–344, covering several subclasses of lipids.

In our study, we chose a focused approach, looking at the molecular species of the most abundant lipid classes, MGDG and DGDG. As there might be differences in the lipid composition of stipe and blade, it was chosen to analyze the different parts separately. The samples were analyzed using a reversed phase (RP)—high performance liquid chromatography (HPLC)-MS/MS method. The separation was mainly based on acyl chain length and degree of unsaturation, as opposed to a lipid head-group approach. This allows for a more detailed investigation of the molecular species within the chosen classes. To the best of our knowledge, this is the first study on the identification of lipid molecular species in *L. hyperborea*. This is the first step towards the future discovery of new bioactive lipids, as well as discovering if *L. hyperborea* is a source for already-identified lipids of interest.

2. Materials and Methods

2.1. Sampling and Pretreatment

Samples of blade and stipe from *L. hyperborean* (two plants) harvested in the Vikna-Horta area, Norway, in May 2018, were provided and identified by DuPont Nutrition & Biosciences Biopolymer AS (Sandvika, Norway). The samples were vacuum packed and shipped immediately and kept at 4 °C during shipping. Upon arrival, the samples were frozen at –24 °C until pretreatment could begin. The sea temperature in May 2018 was between 7.4–9.1 °C, measured at observation station Heidrun [28]. The samples were pretreated by thawing, cutting (<1 cm³ pieces), freezing with liquid nitrogen and freeze drying (Alpha 2-4 LD plus, Martin Christ Gefriertrocknungsanlagen GmbH, Osterode am Harz, Germany). The freeze-dried material was milled with a Retsch SM 2000 (Retsch GmbH, Haan, Germany) to a fine powder (<1 mm²). The two plants were pooled to one sample, but the blades and the stipes were analyzed separately.

2.2. Lipid Extraction and Determination of Total Lipid Content

Lipids were extracted on two separate occasions, one for fatty acid profile determination (gas chromatography-mass spectrometry) and one for lipidomic analysis (liquid chromatography-tandem mass spectrometry). Four technical replicates were used for both stipe and blade. In addition, two blanks (one for stipe and one for blade) were used for each analysis. The extraction procedure was the same on both occasions, as outlined below. The lipids were extracted with a modified Folch's method [29], as previously reported [30]. In short, for each replicate, 5.0 g of pulverized seaweed and 100 mL chloroform:methanol (2:1 *v/v*) were added to a 250 mL borosilicate flask, and shaken at 220 rpm for 20 min on an orbital shaker (PSU-10i, Biosan, Riga, Latvia). The samples were transferred to separatory funnels and phase separation was induced by addition of 20 mL 0.9% (*v/v*) NaCl in LC-MS

grade water. The samples were gently shaken, and the organic phases removed after 20 min. The aqueous phases were extracted twice with 66 mL chloroform. The organic phases of each sample were combined and evaporated at 40 °C with a vacuum evaporator (Q-101, Buchi Labortechnik AG, Flawil, Switzerland). The combined samples were redissolved in 1.0 mL chloroform before being transferred to microtubes and centrifuged on a Sigma 1–14 microcentrifuge (Sigma Laborzentrifugen GmbH, Osterode, Germany) at 16,112 g for 5 min. The supernatants were transferred to microtubes and evaporated, and the total lipid contents were determined gravimetrically. The samples were redissolved in 1.0 mL chloroform and transferred to vials for storage (−24 °C) prior to solid phase extraction (SPE).

2.3. Solid Phase Extraction

Solid phase extraction (SPE) was carried out to separate the polar lipids (PL) from the neutral lipids (NL) and the free fatty acids (FFA). The SPE procedure was carried out, as previously reported [31,32], on a liquid-handling robot (Gilson, GX-271, ASPEC, Middleton, WI, USA), with a method based on procedures by Pinkart et al. [33] and Ruiz et al. [34]. In short, 500 µL of the samples were applied to pre-conditioned (7.5 mL heptane) aminopropyl SPE columns (Chromabond, 500 mg, 3 mL, Machery-Nagel, Düren, Germany). The NL, FFA and PL fractions were sequentially eluted with 5 mL of chloroform, diethyl ether:acetic acid (98:2, *v/v*) and methanol, respectively. The flow was 1 mL min^{−1}. The fractionated samples were evaporated at 40 °C under N₂, and redissolved in 1 mL chloroform:methanol (1:1). The samples were filtered with a 0.2 µm Millex[®]—FG syringe filter with Hydrophobic Fluoropore[™] (PTFE) membrane (Merck KGaA, Darmstadt, Germany). Each filter was pre-conditioned with 1–2 mL of chloroform:methanol (1:1) before the samples were applied. The filtered samples were stored at −24 °C until further analysis by HPLC-MS/MS or GC-MS.

2.4. Analysis of Fatty Acid Methyl Esters by Gas Chromatography-Mass Spectrometry

The lipids extracted for GC-MS analysis were esterified/transesterified to fatty acid methyl esters (FAME), as previously reported [30]. Four technical replicates were used for each fraction of blade and stipe, respectively. In brief, the NL and PL fractions were dissolved in 3 mL n-heptane and 1.5 mL of a 3.3 mg mL^{−1} sodium methoxide methanol solution was added. The samples were shaken for 30 min at 350 rpm (Biosan Ltd., PSU-10i, Riga, Latvia) and left to settle for 10 min before the heptane phases were transferred to vials. The FFA fraction was dissolved in 1 mL 14% boron trifluoride-methanol solution (Merck KGaA, Darmstadt, Germany) and heated in a water bath at 70 °C for 5 min. n-heptane (1 mL) was then added, and the samples were mixed with a vortex mixture and left to settle. The heptane phases were transferred to vials. The samples were stored at −24 °C prior to GC-MS analysis.

The fatty acid profiles were determined using an Agilent 6890 series GC (Agilent Technology, Santa Clara, CA, USA) with a CTC PAL autosampler coupled to an Autospec Ultima triple sector mass spectrometer with EBE geometry (Micromass Ltd. Manchester, England), with an electron ionization ion source (70 eV), as described previously [32]. A 1.0 µL injection volume was used with a split ratio of 1:10. A fused silica stationary phase with 90% biscyanopropyl and 10% phenylcyanopropyl polysiloxane was used (60 m × 0.24 mm, 0.2 µm film thickness, Rtx-2330, Restek Corporation, Bellefonte, PA, USA). The carrier gas (Helium, 99.99990%, AGA, the Linde Group, Munich, Germany) had a constant flow of 1.0 mL min^{−1}. The column oven temperature program started at 65 °C and was held for 3 min, was then increased to 150 °C at 40 °C min^{−1}, which was held for 13 min, then increased to 151 °C in half a minute, was held for 20 min, then increased to 230 °C by 2 °C min^{−1}, was held for 10 min, and finally increased to 240 °C by 50 °C min^{−1} and was held for 3.7 min.

The EI ion source produced 70 eV electrons in positive mode at 250 °C. A scan range of *m/z* 40–600 was used with a 0.3 s scan time and 0.2 s interscan delay. The resolution of

the MS was set to 1000. MassLynx software version 4.0 (Waters, Milford, MA, USA) was used to process the data.

Identification was achieved through a combination of library searches (NIST 2017 Mass spectral Library v.2.2.; Gaithersburg, MD, USA) and retention time comparison with standards. A FAME mix with 37 components (Food Industry FAME MIX, Restek Corporation, Bellefonte, PA, USA) as well as the following individual standards were used: nonadecanoic acid methyl ester (C9:0, Fluka, now Merck KGaA, Darmstadt, Germany), *cis*-7-hexadecenoic acid methyl ester (C16:1*cis*-7), *cis*-9-heptadecenoic acid methyl ester (C17:1*cis*-9), *cis*-11-octadecenoic acid methyl ester (C18:1*cis*-11), *cis*-9-eicosaenoic acid methyl ester (C20:1*cis*-9), all-*cis*-6,9,12,15-octadecatetraenoic acid methyl ester (C18:4*cis*-6,9,12,15), all-*cis*-8,11,14,17-eicosatetraenoic acid methyl ester (C20:4*cis*-8,11,14,17), all-*cis*-7,10,13,16,29-docosapentaenoic acid methyl ester (C22:5*cis*-7,10,13,16,19), and hexacosanoic acid methyl ester (C26:0), all from Larodan AB (Solna, Sweden). Relative fatty acid profiles were made for each fraction of blade and stipe.

2.5. Analysis of Glyceroglycolipids by High Performance Liquid Chromatography-Tandem Mass Spectrometry

A method for identification of glyceroglycolipids in seaweed was developed. The lipids were separated on a RP Kinetex[®] 2.6 μm C18 100 Å column (150 mm \times 2.1 mm, Phenomenex, Torrance, CA, USA) on a HPLC (Ultimate 3000, Thermo Fisher Scientific, Waltham, MA, USA). A C18 guard column was used (SecurityGuard ULTRA for 2.1 mm ID columns, Phenomenex, Torrance, CA, USA). The mobile phase composition was as follows: 100% water, B: 100% chloroform, C: 40 mM sodium acetate in methanol, and D: 100% methanol. For sodium adduct formation purposes 1% (*v/v*) of the mobile phase was C, at all times. The mobile phase gradient started with 20% A, 1% C and 79% D and increased linearly to 1% B, 1% C and 98% D over 200 min, followed by a linear change to 5% B, 1% C, 94% D over 40 min, then returned quickly (over 5 min) to the initial mobile phase conditions, which then was held for 5 min. The flow rate was 0.4 mL min⁻¹. The sample injection volume was 2.0 μL . Four technical replicates were used for each fraction of stipe and blade, respectively. The column oven was set at 30 °C and the sample chamber was held at 4 °C. An ESI-linear ion trap mass spectrometer (LTQ XL, Thermo Fisher Scientific, Waltham, MA, USA) was used for fragmentation and detection. The transfer capillary had a temperature of 275 °C with a sweep and auxiliary gas flow of 5.00 arb. units and a sheath gas flow of 40.00 arb. units. The MS was operated in positive mode with an electrospray voltage of 4.5 kV, a scan range of *m/z* 50 to 2000 in full scan, and a normalized collision energy (CE) of 75.00 in MS/MS mode. Both the HPLC and the MS were controlled by Xcalibur 2.2 SP1.48 (Thermo Fisher Scientific, Waltham, MA, USA).

The analysis method was evaluated with MGDG and DGDG standards (C16:0, C18:0 mixes, Larodan AB, Solna, Sweden). Both the expected retention times and fragmentation patterns of MGDG and DGDG were confirmed. No limit of detection was established for the method, but preliminary testing showed detection of 10 ng mL⁻¹ DGDG standard with signal to noise at 77 (calculated by Xcalibur software with no peak smoothing).

2.6. Data Analysis

The 47 identified fatty acids from the GC-MS profile corresponded to 32 carbon-to-double-bond-equivalent ratios (C:DBE), which again corresponded to 544 possible acyl chain pairs for each diacylglycerol. Reconstructed ion chromatograms (RIC) were made from the MS full scans of the lipid fractions for each of the predicted lipids. When a peak was present in the chromatogram, a limited-time-window two-stage full scan (MS/MS) was set up for this particular *m/z*. The glyceroglycolipids were identified through their MS/MS fragmentation patterns as discussed in the results and discussion section. All the data analysis was conducted manually using Xcalibur 2.2 SP1.48 (Thermo Fisher Scientific, Waltham, MA, USA). Due to the limitations with MS/MS scan range in a linear ion trap, MGDG with a predicted parent *m/z* higher than 889.8 Da could not be analyzed.

The percentages of the acyl chains with a given number of carbon atoms (or DBE) were calculated for MGDG and DGDG in blade and stipe separately. The percentages, thus, represent the fraction of identified acyl chains with a given C or DBE, not the quantity of the lipids.

3. Results and Discussion

3.1. Total Lipid Content and Fatty Acid Profile

The total lipid contents were determined gravimetrically to be $1.3 \pm 0.1\%$ ($n = 4$) and $1.1 \pm 0.1\%$ ($n = 4$) for blade and stipe, respectively. The lipid extracts were fractionated into neutral lipids (NL), free fatty acids (FFA) and polar lipids (PL). In blade, $18.2 \pm 0.8\%$ of the fatty acids were in the NL fraction, $58.7 \pm 0.8\%$ in the FFA fraction and $23.1 \pm 0.5\%$ in the PL fraction. In stipe, the distribution was $36.5 \pm 1.2\%$ NL, $10.3 \pm 0.6\%$ FFA and $53.2 \pm 1.3\%$ PL. In blade and stipe of *L. hyperborea*, a total of 47 fatty acids were identified (Supplementary Materials, Table S1). The fatty acid profile of *L. hyperborea* was used to predict the mass of MGDG and DGDG molecular species. These species were subsequently searched for by HPLC-MS/MS analysis. The profiles of all fractions, both in blade and stipe, were mainly predominated by the same nine fatty acids. The exception being the FFA fraction of stipe which, in addition, had a high content ($5.9 \pm 0.3\%$) of stearic acid (C18:0). Of these nine fatty acids: two were saturated; myristic acid (C14:0) and palmitic acid (C16:0), two were monounsaturated: palmitoleic acid (C16:1n-7) and oleic acid (C18:1n-9), and five were polyunsaturated fatty acids: linoleic acid (C18:2n-6), α -linolenic acid (C18:3n-3), stearidonic acid (SDA, C18:4n-3), arachidonic acid (C20:4n-6) and eicosapentaenoic acid (EPA, C20:5n-3). This is in agreement with what has been reported previously for *L. hyperborea* [32,35–37]. In the PL fractions of both blade and stipe, these nine fatty acids constituted more than 95%. However, considerable differences between the content of these fatty acids were seen between stipe and blade (Table S1).

3.2. Identification of Glyceroglycolipids by HPLC-ESI-MS/MS Analysis

The molecular species of MGDG and DGDG were separated mainly based on the total number of carbon atoms (C) and the double bond equivalents (DBE) in the acyl chains. For the identification of the glyceroglycolipids, a combination of retention times and fragmentation characteristics due to collision-induced dissociation (CID) was used. Both MGDG and DGDG were detected as $[M + Na]^+$ adducts. CID of MGDG sodium adducts resulted in the neutral loss of one hexose residue (loss of 162 Da), and the formation of a characteristic headgroup product ion at m/z 243 corresponding to $[C_9H_{16}O_6 + Na]^+$ [38]. CID of sodium adducts of DGDG resulted in the neutral loss of one and, sometimes, two hexose residue(s), losses of 162 Da and 324 Da, respectively. Additionally, the formation of characteristic headgroup product ions at m/z 347 $[Hex_{2res} + Na]^+$, m/z 365 $[Hex_2 + Na]^+$ and m/z 405 $[C_{15}H_{26}O_{11} + Na]^+$ were observed, agreeing with published data [38]. The acyl chains were identified from the product ions resulting from the loss of the acyl chains as neutral carboxylic acids, as well as from the product ions resulting from a combined loss of a neutral carboxylic acid and a hexose residue. The position of the acyl chains on MGDG and DGDG can be determined from the intensities of the product ions corresponding to loss of the acyl chains as neutral carboxylic acids [39]. In ESI-MS/MS of MGDG and DGDG, the most intense product ion in the mass spectra corresponds to loss of the *sn*-1 bound acyl chain [39]. Several molecular species with the same carbon-to-double-bond-equivalent ratio (C:DBE) indicated for the acyl chains were identified in sequentially eluting peaks, indicating different isomers. These isomers could be double bond positional isomers, *cis/trans*-isomers or due to branching or cyclic formation on the acyl chains. Illustrative MS/MS mass spectra for MGDG and DGDG are shown in Figure 1. While the fatty acid profile was used to predict the molecular species of the glyceroglycolipids, some of the identified glyceroglycolipids had acyl chains not found in the profile. This occurred as the CID of a predicted parent ion resulted in product ions for several acyl pairs, not only the predicted combination(s). The reason for this is because molecular species of MGDG or

DGDG with the same total number of C:DBE co-elute. For example, the predicted MGDG molecular species with C:DBE 34:4 and parent ion m/z 773.51 (Table S2) was based on the predicted combination of a C18:4 and a 16:0, or C20:4 and C14:0 fatty acid. However, we also identified fragments corresponding to C18:1 and C16:3. A fragment corresponding to a C16:3 fatty acid was not expected based on the fatty acid profile.

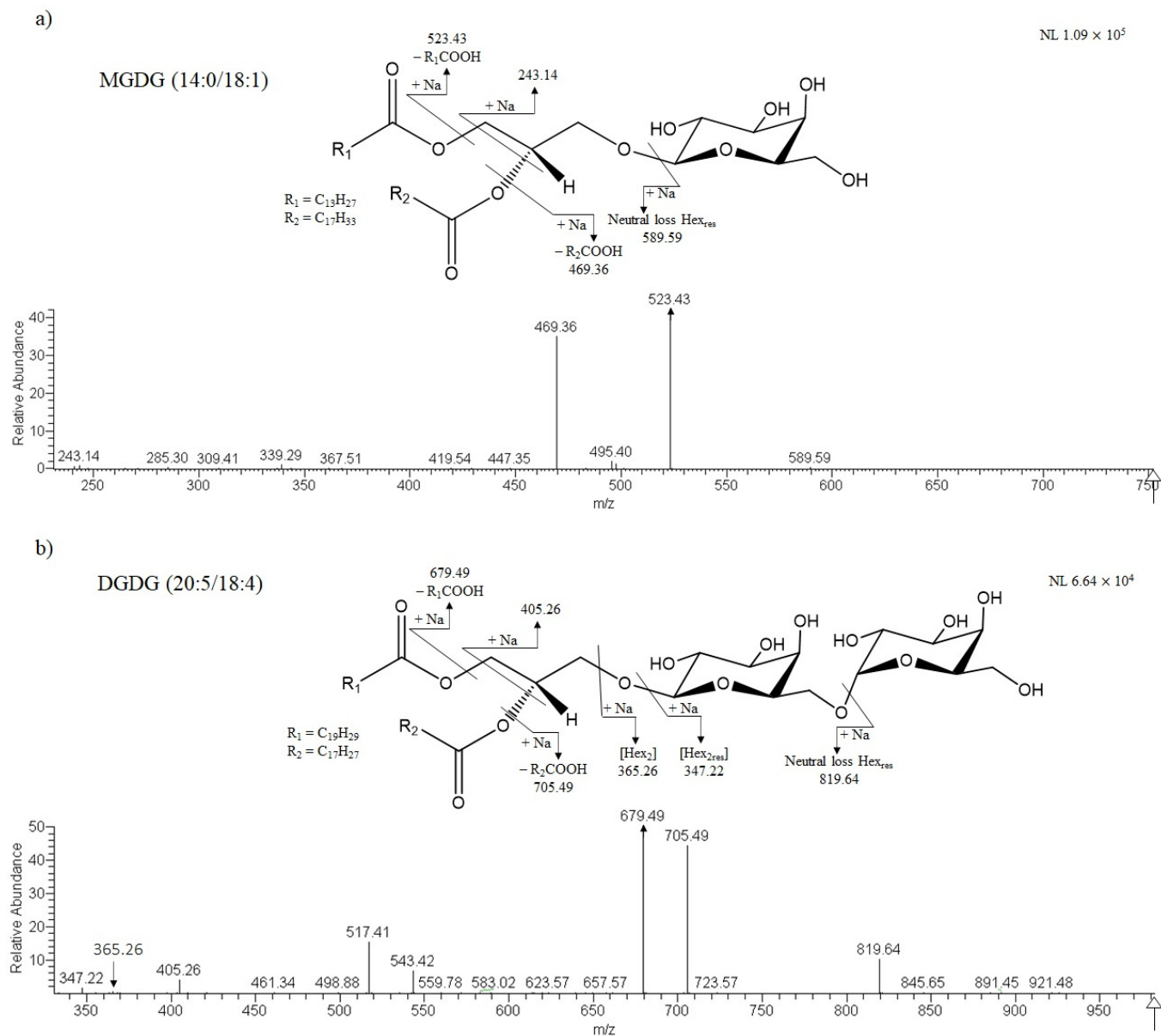


Figure 1. Illustrative tandem mass spectra of (a) Monogalactosyldiacylglycerol (MGDG) (14:0/18:1) at m/z 751.53 and (b) Digalactosyldiacylglycerol (DGDG) (20:5/18:4) at m/z 981.56, as $[M + Na]^+$ ions. In addition to the product ions indicated in (b), the MS/MS spectra for DGDG (20:5/18:4) also showed clear product ions for the combined neutral loss of a hexose residue and each of the acyl chains as neutral carboxylic acids. These losses correspond to product ions at m/z 517.41 (-Hexose residue and R₁COOH) and m/z 543.42 (-Hexose residue and R₂COOH). NL: normalization level (base peak intensity).

3.3. Characterization of Mono- and Digalactosyldiacylglycerols in *Laminaria Hyperborea*

The NL, FFA and PL fractions were all checked for predicted glyceroglycolipids. The NL and FFA fractions were not found to contain any of the predicted MGDG or DGDG, as expected, since glyceroglycolipids should only be found in the PL fraction. All

further presented results are, therefore, pertaining to this fraction. A total of 103 molecular species of MGDG and 66 species of DGDG were identified in blade from *L. hyperborea*. In stipe, 161 and 136 molecular species of MGDG and DGDG were identified, respectively. Detailed information on the identified glyceroglycolipid molecular species can be found in Supplementary Materials (Tables S2–S5). The most abundant molecular species of each identified total C:DBE can be seen in Tables 1 and 2 for MGDG and DGDG, respectively.

The molecular species of MGDG and DGDG had acyl chains varying from 11 to 25 carbon atoms and 0 to 9 DBE. A higher number of molecular species of MGDG (264) were identified compared to DGDG (202). This is expected as only selected species of MGDG are used for DGDG synthesis [40]. It has been reported that MGDG has a higher proportion of PUFA compared to that of DGDG [41], yet we find no clear evidence of this in our data. When defining PUFA as one of the acyl chains having two DBE or more, the proportion of PUFA was between 55–70% of identified lipids in MGDG and DGDG, both in blade and stipe. However, it must be considered that these numbers are based on the number of identified glyceroglycolipids, not their quantity.

A higher number of molecular lipid species was found in stipe (297 in total) compared to blade (169 in total). We have no clear explanation for this. However, *L. hyperborea* grows a new blade in spring, and while most of the nutrients are transferred to the new blade, the details of this process are not known. Despite this, the total number of C:DBE ratios identified in blade and stipe was similar within MGDG (29 vs 31 in blade and stipe, respectively) and DGDG (22 vs. 19 in blade and stipe, respectively). While a larger number of isomers were identified in stipe, the most abundant acyl chain pairs for each C:DBE ratio was largely the same in both blade and stipe (Tables 1 and 2). In MGDG, 18 out of the 25 C:DBE ratios had the same acyl chain pair as the most abundant in blade and stipe. While in DGDG, 15 out of 18 were the same acyl chain pairs. Overall, most of the glyceroglycolipids seem to be in common for both blade and stipe.

Table 1. Monogalactosyldiacylglycerol (MGDG) lipids identified in blade and stipe of *Laminaria hyperborea*.

C:DBE	<i>m/z</i> [M + Na] ⁺	Bioactivity	MGDG					
			Blade			Stipe		
			Peaks	Isomers	Acyl Chain Pair ^a	Peaks	Isomers	Acyl Chain Pair ^a
28:0	697.48					1	2	14:0/14:0
30:0	725.51		1	1	14:0/16:0	1	1	14:0/16:0
30:1	723.50	AT [11]	1	2	14:0/16:1	1	2	14:0/16:1
31:1	737.51					2	4	14:0/17:1
32:1	751.53		2	3	14:0/18:1	1	2	14:0/18:1
32:2	749.51		1	2	14:0/18:2	2	3	14:0/18:2
32:3	747.50		1	1	14:0/18:3	4	11	14:0/18:3
33:1	765.54		1	3	15:0/18:1	2	5	15:0/18:1
34:1	779.56	I [42], AA [7]	1	1	16:0/18:1	1	2	16:0/18:1
34:2	777.54					2	2	16:0/18:2
34:3	775.53		1	1	16:0/18:3	6	14	16:2/18:1
34:4	773.51	AI [15] ^c	2	7	18:4/16:0	6	15	14:0/20:4
34:5	771.50	AI [43] ^d	3	7	16:1/18:4	2	4	20:5/14:0
34:6	769.48		1	2	16:2/18:4			
34:7	767.69					4	9	14:0/20:7 or 15:7/19:0 ^b
34:8	765.54		1	1	16:4/18:4			
35:1	793.58					1	3	17:0/18:1
36:1	807.59					3	8	18:0/18:1
36:2	805.58		2	5	18:1/18:1	3	6	18:1/18:1
36:3	803.56		1	1	18:2/18:1	4	6	18:2/18:1
36:4	801.54		1	1	18:3/18:1			

Table 1. Cont.

MGDG								
C:DBE	<i>m/z</i> [M + Na] ⁺	Bioactivity	Blade			Stipe		
			Peaks	Isomers	Acyl Chain Pair ^a	Peaks	Isomers	Acyl Chain Pair ^a
36:5	799.53	AI [15] ^d	4	11	18:4/18:1	5	11	20:5/16:0
36:6	797.51		3	8	20:5/16:1	9	26	18:4/18:2
36:7	795.59		2	3	18:4/18:3	6	12	18:4/18:3
36:8	793.48		1	1	18:4/18:4	7	13	18:4/18:4
36:9	791.58		2	3	18:4/18:5	5	10	20:5/16:4
38:5	827.56		3	6	20:4/18:1	8	21	20:4/18:1
38:6	825.54		1	1	20:4/18:2	6	18	20:5/18:1
38:7	823.53	AI [43]	6	12	20:5/18:2	6	13	20:5/18:2
38:8	821.51	AI [16], AF [19]	3	6	20:5/18:3	2	4	20:5/18:3
38:9	819.50	AI [16], AF [19]	1	1	20:5/18:4	1	1	20:5/18:4
40:6	853.58		1	2	22:5/18:1			
40:8	849.54	AI [15]	4	7	20:4/20:4	4	7	20:4/20:4
40:9	847.53		2	3	20:4/20:5	4	5	20:4/20:5
40:10	845.51	AI [15]	1	1	20:5/20:5	1	1	20:5/20:5

^a Most abundant acyl chain pair where the *sn*-1 acyl chain had the highest intensity in the mass spectra, for that C:DBE. ^b The loss of a neutral fatty acid in the mass spectra corresponds to two different fatty acids with the same mass. ^c molecular species indicated for blade only. ^d molecular species indicated for stipe only. AA: anti-algal, AI: anti-inflammatory, AF: anti-fungal, AT: anti-tumor, C: number of carbon atoms in the acyl chains, DBE: double bond equivalents, I: mammalian DNA polymerase α inhibitor.

Table 2. Digalactosyldiacylglycerol (DGDG) lipids identified in blade and stipe of *Laminaria hyperborea*.

DGDG								
C:DBE	<i>m/z</i> [M + Na] ⁺	Bioactivity	Blade			Stipe		
			Peaks	Isomers	Acyl Chain Pair ^a	Peaks	Isomers	Acyl Chain Pair ^a
30:1	885.64		1	2	14:0/16:1	1	2	14:0/16:1
32:1	913.67		1	2	14:0/18:1	1	2	14:0/18:1
32:2	911.65		1	2	14:0/18:2	3	4	14:0/18:2
32:3	909.64	AT [11]	1	1	14:0/18:3			
34:1	941.70		1	2	16:0/18:1	1	2	16:0/18:1
34:2	939.69		2	4	16:0/18:2	2	2	16:1/18:1
34:3	937.67					7	13	16:1/18:2
34:4	935.72		2	5	18:4/16:0	6	14	20:4/14:0
34:5	933.56	AI [14]	2	2	20:5/14:0			
35:1	955.64		1	2	17:0/18:1	1	3	17:0/18:1
36:1	969.65		1	1	18:1/18:0			
36:2	967.72		1	2	18:1/18:1	1	3	18:1/18:1
36:3	965.70		1	2	18:2/18:1	3	6	18:2/18:1
36:4	963.60		2	5	18:3/18:1	8	17	18:3/18:1
36:5	961.59	AI [15]	3	7	20:5/16:0	3	6	20:5/16:0
36:6	959.57	AI [44]	1	1	20:5/16:1	6	12	20:5/16:1
36:7	957.65		3	5	18:3/18:4	2	5	20:5/16:2
36:8	955.54		1	1	18:4/18:4			
38:5	989.62		3	7	20:4/18:1	4	7	20:4/18:1
38:6	987.60		2	3	20:5/18:1	5	14	20:5/18:1
38:7	985.68	AI [43]	2	6	20:5/18:2	6	17	20:5/18:2
38:8	983.67		2	3	20:5/18:3	3	6	20:5/18:3
38:9	981.65		1	1	20:5/18:4	1	1	20:5/18:4

^a Most abundant acyl chain pair where the *sn*-1 acyl chain had the highest intensity in the mass spectra, for that C:DBE. AI: anti-inflammatory, AT: anti-tumor, C: number of carbon atoms in the acyl chains, DBE: double bond equivalents.

3.3.1. Most Abundant Glyceroglycolipid Species

The most abundant lipid species can be seen from the total ion chromatograms (TIC) of blade and stipe (Figure 2). The most abundant acyl pairs in these peaks correspond to MGDG(18:4/18:4), MGDG(20:5/18:4), DGDG(16:0/18:1) and DGDG(20:5/18:4) in blade only, and MGDG(14:0/18:2), MGDG(16:0/18:1), and MGDG and DGDG(14:0/18:1) in both blade and stipe. Studies of the lipid content of *Sargassum horneri* [45], *S. thunbergii* [19], *Fucus spiralis* [16], *F. vesiculosus* [26] and *Saccharina latissima* [27,46] show that there is a large variation in the most abundant species of MGDG and DGDG in brown seaweed. This concurs with numerous studies that have shown that the fatty acid distribution in seaweed varies substantially with season, environmental factors and harvesting location (see e.g., [47–50]). A similar variety can be expected for the lipid profiles as well, and some studies have shown seasonal variation in glyceroglycolipids contents in seaweed [26,27,51].

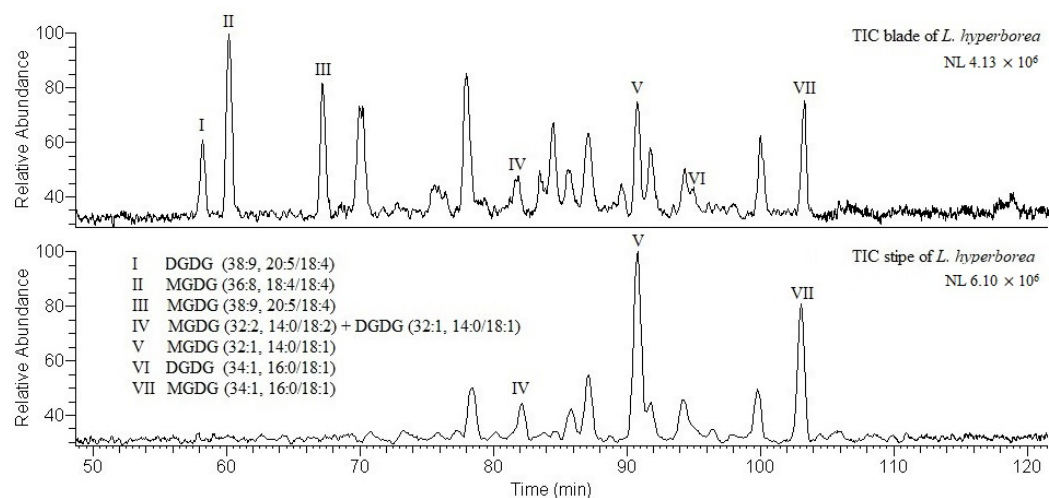


Figure 2. Total ion chromatogram (TIC) of blade (**top**) and stipe (**bottom**) of *Laminaria hyperborea*. The molecular species indicated after the carbon-to-double-bond-equivalent ratio (C:DBE) was the most abundant species for that C:DBE. MGDG: monogalactosyldiacylglycerol, DGDG: digalactosyldiacylglycerol, NL: normalization level (base peak intensity).

From these chromatograms (Figure 2), we can deduce that MGDG and DGDG might be more abundant in blade than in stipe, though this is not conclusive. Previous studies have shown that the abundance of pigments related to photosynthesis, such as chlorophyll *a* and *c*, fucoxanthin and β -carotene, are more abundant in blades than in stipes of *L. hyperborea* [35,52]. This indicates that photosynthesis, and, thus, lipids related to photosynthetic membranes should be more prevalent in the blades.

The Distribution of Carbon and Double Bond Equivalents in the Acyl Chains

Acyl chains with 16, 18 or 20 carbon atoms were the most common in both MGDG and DGDG from blade and stipe (Figure 3a). For MGDG and DGDG, in both blade and stipe, these three acyl chain lengths constituted between 80 and 92% of the acyl chains. This concurs with the fatty acid profile (Table S1).

The number of carbon atoms in the acyl chain in the *sn*-2 position is indicative of the synthesis pathway. The "prokaryotic pathway," which occurs in the plastids envelope, is indicated by 16 carbon atoms in the *sn*-2 position. An 18-carbon atom chain indicates the "eukaryotic pathway", which relies on precursors from the endoplasmic reticulum (ER) being transferred to the envelope [40,53]. Our results indicate that MGDG and DGDG are synthesized in both the plastids and the ER; however, the number of molecular species identified with 18 carbons in the *sn*-2 position was roughly 3 times higher than those with 16.

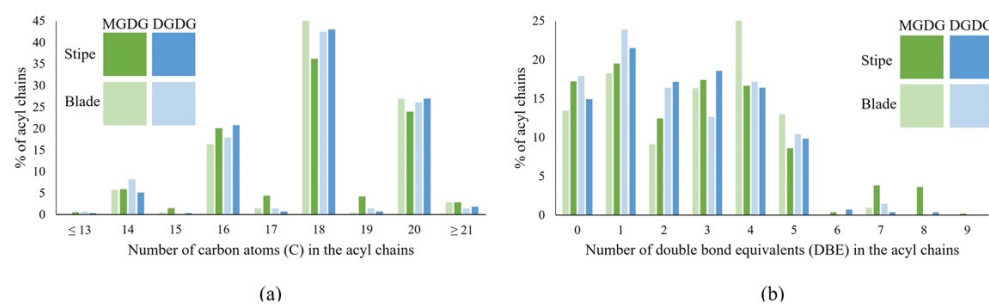


Figure 3. Distribution of (a) the number of carbon atoms (C), and (b) the double bond equivalents (DBE) in the acyl chains of mono- and digalactosyldiacylglycerols (MGDG and DGDG, respectively) for blade and stipe from *Laminaria hyperborea*. Note that this figure represents the number of identified acyl chains with a given C or DBE, not the quantity of the lipids.

Overall, the lower numbers of DBE were the most common, with 0 to 5 DBE accounting for more than 90% of the acyl chains (Figure 3b). Interestingly, the samples differed in which DBE were the most common. For both MGDG and DGDG in stipe, and DGDG in blade, it was 1 DBE. In MGDG in blade it was 4 DBE. Overall, for MGDG, 4 and 5 DBE were more common in blade than in stipe samples with 1.7- and 1.5-times higher occurrences. For DGDG, the ratio between blade and stipe was almost equal with ratios of 1.0 and 1.1 for 4 and 5 DBE, respectively. This difference observed in MGDG was also reflected in the fatty acid profile of the PL fractions. Compared to stipe, the PL fraction of blade had higher occurrences of 4 and 5 double bonds, mainly due to considerably higher amounts of SDA and EPA, and lower of 0 and 1, due to lower amounts of myristic, palmitic and oleic acid (Table S1, Figure S1).

In stipe, DGDG generally had a lower occurrence of the higher numbers of DBE (≥ 6 , 1% compared to 8% in MGDG). In blade, the difference between MGDG and DGDG was smaller, with both having less than 1% of DBE ≥ 6 . In the fatty acid profile, more than 5 double bonds were not found for any fatty acid in the PL fractions.

A scrutiny of the DBE distribution for the three most common acyl chain lengths showed differences in the occurrences of DBE (Figure 4). As expected, the shorter C16 chains were the least unsaturated and were predominated by the lower number of DBE (0–1), the C18 chains mostly had medium numbers of DBE (1–4) and the longer C20 chains were the most unsaturated, with higher numbers of DBE (>3).

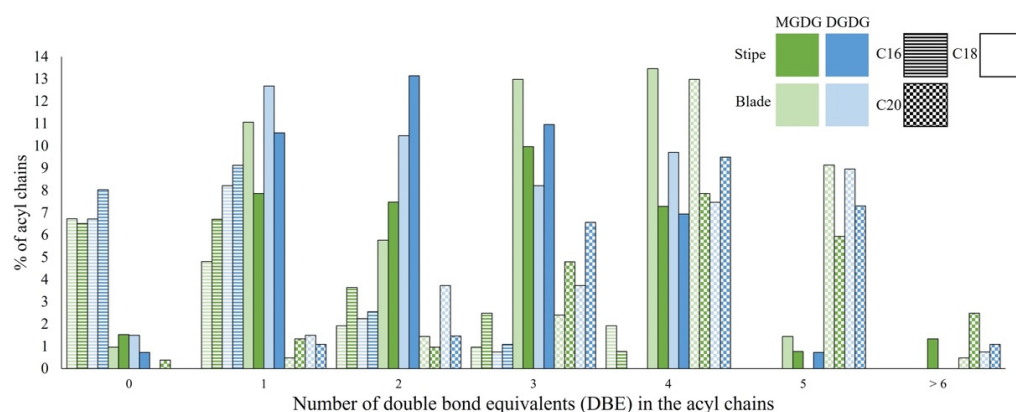


Figure 4. Distribution of the double bond equivalents (DBE) of the C16 (striped), C18 (no pattern) and C20 (chequered) acyl chain for mono- and digalactosyldiacylglycerols (MGDG and DGDG, respectively) of blade and stipe from *Laminaria hyperborea*. Note that this figure represents the number of identified acyl chains with a given DBE, not the quantity of the lipids.

Overall, the distribution of acyl chains and double bond equivalents showed only minor differences between stipe and blade and MGDG and DGDG. However, the most

common DBE in MGDG in blade was 4, while in DGDG in blade, as well as in MGDG and DGDG in stipe, it was 1. Utilizing only the blades can, thus, provide a higher percentage of unsaturated lipids.

4. Conclusions

This study highlights the potential of *Laminaria hyperborea* as a source of valuable glyceroglycolipids. Over 150 molecular species of MGDG and DGDG were identified in blade and stipe, each, from *L. hyperborea*. There were clear differences in the glyceroglycolipid composition of blade and stipe. The most abundant species in blade were MGDG and DGDG (20:5/18:4, 14:0/18:1), MGDG (18:4/18:4, 14:0/18:2, 16:0/18:1) and DGDG (16:0/18:1). In stipe, the most abundant species were MGDG (14:0/18:2, 16:0/18:1), and MGDG and DGDG (14:0/18:1). Acyl chains with 16, 18 and 20 carbon atoms were the most common in the glyceroglycolipids from both blade and stipe. However, the distribution of DBE varied. In MGDG in blade, 4 DBE were the most common, while 1 DBE were the most common in stipe and DGDG in blade. Several of the identified molecular species of MGDG and DGDG have previously been reported to display bioactive properties. Moreover, these findings support the supposition that there is great potential for further valorization of biomass from *L. hyperborea*. As further research into the bioactivity of the different molecular species of MGDG and DGDG progress, the need for more comprehensive studies on the content and variability of these lipids in seaweeds is of importance.

Supplementary Materials: The following supporting information can be downloaded at: <https://www.mdpi.com/article/10.3390/appliedchem2040013/s1>, Table S1: Fatty acid distribution in the neutral lipid (NL), free fatty acid (FFA) and polar lipid (PL) fractions of blade and stipe from *Laminaria hyperborea*, Table S2: Molecular species of monogalactosyldiacylglycerol in blade from *Laminaria hyperborea*, Table S3: Molecular species of digalactosyldiacylglycerol in blade from *Laminaria hyperborean*, Table S4: Molecular species of monogalactosyldiacylglycerol in stipe from *Laminaria hyperborean*, Table S5: Molecular species of digalactosyldiacylglycerol in stipe from *Laminaria hyperborean*. Figure S1: Distribution of double bounds for the fatty acids in the polar lipid (PL) fraction of stipe and blade from *Laminaria hyperborea*.

Author Contributions: Conceptualization, L.F., H.D., C.F.N.-A. and D.E.; methodology, L.F., H.D. and D.E.; formal analysis, L.F.; investigation, L.F.; resources, L.F., H.D. and D.E.; data curation, L.F.; writing—original draft preparation, L.F.; writing—review and editing, L.F., H.D., C.F.N.-A. and D.E.; visualization, L.F.; supervision, H.D. and D.E.; project administration, D.E.; funding acquisition, D.E. All authors have read and agreed to the published version of the manuscript.

Funding: This research was funded by the Norwegian University of Life Sciences.

Institutional Review Board Statement: Not applicable since the study did not involve humans or animals.

Informed Consent Statement: Not applicable since the study did not involve humans.

Data Availability Statement: Data are available from the corresponding author upon reasonable request.

Acknowledgments: A special thank you to MSc student Ingeborg Natvik for the sample preparation of FAME samples. The marine alga *Laminaria hyperborea* was used in this study. The specimens were kindly provided by DuPont Nutrition & Biosciences Biopolymer (Sandvika, Norway). We would also like to thank Erling Svensen for allowing us to use his beautiful picture of *L. hyperborea* for the graphical abstract.

Conflicts of Interest: No conflict, informed consent, or human or animal rights are applicable to this study.

References

1. Gundersen, H.; Christie, C.H.; de Wit, H.; Norderhaug, K.M.; Bekkby, T.; Walday, M.G. *Utredning om CO₂-Opptak i Marine Naturtyper [CO₂ Uptake in Marine Habitats—An Investigation]*; Technical Report; Norwegian Institute for Water Research (NIVA): Oslo, Norway, 2011.
2. Statistics Norway. 12847: Catch, by Landing County and Main Group of Target Species (C) 2014–2019. Statbank Norway. Available online: <https://www.ssb.no/en/statbank/table/12847> (accessed on 8 September 2022).
3. Harwood, J.L. Membrane lipids in algae. In *Lipids in Photosynthesis: Structure, Function and Genetics*; Siegenthaler, P.A., Murata, N., Eds.; Springer: Amsterdam, The Netherlands, 1998; pp. 53–64. [[CrossRef](#)]
4. Hölzl, G.; Dörmann, P. Structure and function of glycolipids in plants and bacteria. *Prog. Lipid Res.* **2007**, *46*, 225–243. [[CrossRef](#)]
5. Bruno, A.; Rossi, C.; Marcolongo, G.; Di Lena, A.; Venzo, A.; Berrie, C.P.; Corda, D. Selective in vivo anti-inflammatory action of the galactolipid monogalactosyldiacylglycerol. *Eur. J. Pharmacol.* **2005**, *524*, 159–168. [[CrossRef](#)] [[PubMed](#)]
6. Lopes, D.; Melo, T.; Meneses, J.; Abreu, M.H.; Pereira, R.; Domingues, P.; Lillebø, A.I.; Calado, R.; Domingues, M.R. A new look for the red macroalga *Palmaria palmata*: A seafood with polar lipids rich in EPA and with antioxidant properties. *Mar. Drugs* **2019**, *17*, 533. [[CrossRef](#)] [[PubMed](#)]
7. Sun, Y.Y.; Wang, H.; Guo, G.L.; Pu, Y.F.; Yan, B.U.; Wang, C.H. Isolation, purification, and identification of anti-algal substances in green alga *Ulva prolifera* for anti-algal activity against the common harmful red tide microalgae. *Environ. Sci. Pollut. Res.* **2016**, *23*, 1449–1459. [[CrossRef](#)]
8. Imbs, T.I.; Ermakova, S.P.; Fedoreyev, S.A.; Anastyuk, S.D.; Zvyagintseva, T.N. Isolation of fucoxanthin and highly unsaturated monogalactosyldiacylglycerol from brown alga *Fucus evanescens* C Agardh and in vitro investigation of their antitumor activity. *Mar. Biotechnol.* **2013**, *15*, 606–612. [[CrossRef](#)]
9. da Costa, E.; Melo, T.; Moreira, A.; Bernardo, C.; Helguero, L.; Ferreira, I.; Cruz, M.; Rego, A.; Domingues, P.; Calado, R.; et al. Valorization of lipids from *Gracilaria* sp. through lipidomics and decoding of antiproliferative and anti-inflammatory activity. *Mar. Drugs* **2017**, *15*, 62. [[CrossRef](#)] [[PubMed](#)]
10. Hossain, Z.; Kurihara, H.; Hosokawa, M.; Takahashi, K. Growth inhibition and induction of differentiation and apoptosis mediated by sodium butyrate in Caco-2 cells with algal glycolipids. *In Vitro Cell. Dev. Biol.-Anim.* **2005**, *41*, 154–159. [[CrossRef](#)] [[PubMed](#)]
11. Kendel, M.; Wielgosz-Collin, G.; Bertrand, S.; Roussakis, C.; Bourgougnon, N.; Bedoux, G. Lipid composition, fatty acids and sterols in the seaweeds *Ulva armoricana*, and *Solieria chordalis* from Brittany (France): An analysis from nutritional, chemotaxonomic, and antiproliferative activity perspectives. *Mar. Drugs* **2015**, *13*, 5606–5628. [[CrossRef](#)]
12. Ulivi, V.; Lenti, M.; Gentili, C.; Marcolongo, G.; Cancedda, R.; Descalzi Cancedda, F. Anti-inflammatory activity of monogalactosyldiacylglycerol in human articular cartilage in vitro: Activation of an anti-inflammatory cyclooxygenase-2 (COX-2) pathway. *Arthritis Res. Ther.* **2011**, *13*, R92. [[CrossRef](#)] [[PubMed](#)]
13. Lenti, M.; Gentili, C.; Pianezzi, A.; Marcolongo, G.; Lalli, A.; Cancedda, R.; Cancedda, F.D. Monogalactosyldiacylglycerol anti-inflammatory activity on adult articular cartilage. *Nat. Prod. Res.* **2009**, *23*, 754–762. [[CrossRef](#)]
14. Banskota, A.H.; Stefanova, R.; Sperker, S.; Lall, S.P.; Craigie, J.S.; Hafting, J.T.; Critchley, A.T. Polar lipids from the marine macroalga *Palmaria palmata* inhibit lipopolysaccharide-induced nitric oxide production in RAW264.7 macrophage cells. *Phytochemistry* **2014**, *101*, 101–108. [[CrossRef](#)] [[PubMed](#)]
15. Banskota, A.H.; Stefanova, R.; Sperker, S.; Lall, S.; Craigie, J.S.; Hafting, J.T. Lipids isolated from the cultivated red alga *Chondrus crispus* inhibit nitric oxide production. *J. Appl. Phycol.* **2014**, *26*, 1565–1571. [[CrossRef](#)]
16. Lopes, G.; Daletos, G.; Proksch, P.; Andrade, P.; Valentão, P. Anti-inflammatory potential of monogalactosyl diacylglycerols and a monoacylglycerol from the edible brown seaweed *Fucus spiralis* Linnaeus. *Mar. Drugs* **2014**, *12*, 1406–1418. [[CrossRef](#)]
17. Plouguerné, E.; Ioannou, E.; Georgantea, P.; Vagias, C.; Roussis, V.; Hellio, C.; Kraffe, E.; Stiger-Pouvreau, V. Anti-microfouling activity of lipidic metabolites from the invasive brown alga *Sargassum muticum* (Yendo) Fensholt. *Mar. Biotechnol.* **2010**, *12*, 52–61. [[CrossRef](#)] [[PubMed](#)]
18. Al-Fadhli, A.; Wahidulla, S.; D'Souza, L. Glycolipids from the red alga *Chondria armata* (Kütz.) Okamura. *Glycobiology* **2006**, *16*, 902–915. [[CrossRef](#)]
19. Kim, Y.H.; Kim, E.H.; Lee, C.; Kim, M.H.; Rho, J.R. Two new monogalactosyl diacylglycerols from brown alga *Sargassum thunbergii*. *Lipids* **2007**, *42*, 395–399. [[CrossRef](#)]
20. Reshef, V.; Mizrahi, E.; Marezki, T.; Silberstein, C.; Loya, S.; Hizi, A.; Carmeli, S. New acylated sulfoglycolipids and digalactolipids and related known glycolipids from cyanobacteria with a potential to inhibit the reverse transcriptase of HIV-1. *J. Nat. Prod.* **1997**, *60*, 1251–1260. [[CrossRef](#)] [[PubMed](#)]
21. Deal, M.S.; Hay, M.E.; Wilson, D.; Fenical, W. Galactolipids rather than phlorotannins as herbivore deterrents in the brown seaweed *Fucus vesiculosus*. *Oecologia* **2003**, *136*, 107–114. [[CrossRef](#)]
22. da Costa, E.; Azevedo, V.; Melo, T.; Rego, A.M.; Evtuguin, D.V.; Domingues, P.; Calado, R.; Pereira, R.; Abreu, M.H.; Domingues, M.R. High-resolution lipidomics of the early life stages of the red seaweed *Porphyra dioica*. *Molecules* **2018**, *23*, 187. [[CrossRef](#)] [[PubMed](#)]

23. Honda, M.; Ishimaru, T.; Itabashi, Y.; Vyssotski, M. Glycerolipid composition of the red macroalga *Agarophyton chilensis* and comparison to the closely related *Agarophyton vermiculophyllum* producing different types of eicosanoids. *Mar. Drugs* **2019**, *17*, 96. [CrossRef]
24. da Costa, E.; Melo, T.; Moreira, A.S.; Alves, E.; Domingues, P.; Calado, R.; Abreu, M.H.; Domingues, M.R. Decoding bioactive polar lipid profile of the macroalgae *Codium tomentosum* from a sustainable IMTA system using a lipidomic approach. *Algal Res.* **2015**, *12*, 388–397. [CrossRef]
25. Kostetsky, E.; Chopenko, N.; Barkina, M.; Velansky, P.; Sanina, N. Fatty acid composition and thermotropic behavior of glycolipids and other membrane lipids of *Ulva lactuca* (Chlorophyta) inhabiting different climatic zones. *Mar. Drugs* **2018**, *16*, 494. [CrossRef] [PubMed]
26. da Costa, E.; Domingues, P.; Melo, T.; Coelho, E.; Pereira, R.; Calado, R.; Abreu, M.H.; Domingues, M.R. Lipidomic signatures reveal seasonal shifts on the relative abundance of high-valued lipids from the brown algae *Fucus vesiculosus*. *Mar. Drugs* **2019**, *17*, 335. [CrossRef] [PubMed]
27. Monteiro, J.P.; Rey, F.; Melo, T.; Moreira, A.S.P.; Arbona, J.F.; Skjermo, J.; Forbord, S.; Funderud, J.; Raposo, D.; Kerrison, P.D.; et al. The unique lipidomic signatures of *Saccharina latissima* can be used to pinpoint their geographic origin. *Biomolecules* **2020**, *10*, 107. [CrossRef] [PubMed]
28. Norwegian Centre for Climate Services. Observations and Weather Statistics. Available online: <https://seklima.met.no/observations/> (accessed on 8 September 2022).
29. Folch, J.; Lees, M.; Stanley, G.H.S. A simple method for the isolation and purification of total lipides from animal tissues. *J. Biol. Chem.* **1957**, *226*, 497–509. [CrossRef]
30. Foseid, L.; Devle, H.; Ekeberg, D. Identification of fatty acids in fractionated lipid extracts from *Palmaria palmata*, *Alaria esculenta* and *Saccharina latissima* by off-line SPE GC-MS. *J. Appl. Phycol.* **2020**, *32*, 4251–4262. [CrossRef]
31. Devle, H.; Ulleberg, E.K.; Naess-Andresen, C.F.; Rukke, E.O.; Vegarud, G.; Ekeberg, D. Reciprocal interacting effects of proteins and lipids during ex vivo digestion of bovine milk. *Int. Dairy J.* **2014**, *36*, 6–13. [CrossRef]
32. Foseid, L.; Devle, H.; Stenström, Y.; Naess-Andresen, C.F.; Ekeberg, D. Fatty acid profiles of stipe and blade from the Norwegian brown macroalgae *Laminaria hyperborea* with special reference to acyl glycerides, polar lipids, and free fatty acids. *J. Lipids* **2017**, *2017*, 1029702. [CrossRef] [PubMed]
33. Pinkart, H.C.; Devereux, R.; Chapman, P.J. Rapid separation of microbial lipids using solid phase extraction columns. *J. Microbiol. Methods* **1998**, *34*, 9–15. [CrossRef]
34. Ruiz, J.; Antequera, T.; Andres, A.; Petron, M.; Muriel, E. Improvement of a solid phase extraction method for analysis of lipid fractions in muscle foods. *Anal. Chim. Acta* **2004**, *520*, 201–205. [CrossRef]
35. Schmid, M.; Stengel, D. Intra-thallus differentiation of fatty acid and pigment profiles in some temperate Fucales and Laminariales. *J. Phycol.* **2015**, *51*, 25–36. [CrossRef] [PubMed]
36. Mæhre, H.K.; Malde, M.K.; Eilertsen, K.E.; Elvevoll, E.O. Characterization of protein, lipid and mineral contents in common Norwegian seaweeds and evaluation of their potential as food and feed. *J. Sci. Food Agric.* **2014**, *94*, 3281–3290. [CrossRef] [PubMed]
37. Van Ginneken, V.J.T.; Helsper, J.P.F.G.; de Visser, W.; van Keulen, H.; Brandenburg, W.A. Polyunsaturated fatty acids in various macroalgal species from North Atlantic and tropical seas. *Lipids Health Dis.* **2011**, *10*, 104. [CrossRef] [PubMed]
38. Maciel, E.; Leal, M.C.; Lillebø, A.I.; Domingues, P.; Domingues, M.R.; Calado, R. Bioprospecting of marine macrophytes using MS-based lipidomics as a new approach. *Mar. Drugs* **2016**, *14*, 49. [CrossRef]
39. Guella, G.; Frassanito, R.; Mancini, I. A new solution for an old problem: The regiochemical distribution of the acyl chains in galactolipids can be established by electrospray ionization tandem mass spectrometry. *Rapid Commun. Mass Spectrom.* **2003**, *17*, 1982–1994. [CrossRef]
40. Block, M.A.; Jouhet, J.; Maréchal, E.; Bastien, O.; Joyard, J. Role of the envelope membranes in chloroplast glycerolipid biosynthesis. In *Photosynthesis. Advances in Photosynthesis and Respiration*; Eaton-Rye, J., Tripathy, B., Sharkey, T., Eds.; Springer: Dordrecht, The Netherlands, 2012; Volume 34, pp. 191–216. [CrossRef]
41. Li-Beisson, Y.; Thelen, J.J.; Fedosejevs, E.; Harwood, J.L. The lipid biochemistry of eukaryotic algae. *Prog. Lipid Res.* **2019**, *74*, 31–68. [CrossRef]
42. Mizushima, Y.; Sugiyama, Y.; Yoshida, H.; Hanashima, S.; Yamazaki, T.; Kamisuki, S.; Ohta, K.; Takemura, M.; Yamaguchi, T.; Matsukage, A.; et al. Galactosyl-diacylglycerol, a mammalian DNA polymerase α -specific inhibitor from a sea alga, *Petalonia bingbamiae*. *Biol. Pharm. Bull.* **2001**, *24*, 982–987. [CrossRef]
43. Banskota, A.H.; Stefanova, R.; Gallant, P.; McGinn, P.J. Mono- and digalactosyldiacylglycerols: Potent nitric oxide inhibitors from the marine microalga *Nannochloropsis granulata*. *J. Appl. Phycol.* **2013**, *25*, 349–357. [CrossRef]
44. Banskota, A.H.; Stefanova, R.; Sperker, S.; Melanson, R.; Osborne, J.A.; O’Leary, S.J. Five new galactolipids from the freshwater microalga *Porphyridium aeruginum* and their nitric oxide inhibitory activity. *J. Appl. Phycol.* **2013**, *25*, 951–960. [CrossRef]
45. Ma, A.C.; Chen, Z.; Wang, T.; Song, N.; Yan, Q.; Fang, Y.C.; Guan, H.S.; Liu, H.B. Isolation of the molecular species of monogalactosyldiacylglycerols from brown edible seaweed *Sargassum horneri* and their inhibitory effects on triglyceride accumulation in 3T3-L1 adipocytes. *J. Agric. Food Chem.* **2014**, *62*, 11157–11162. [CrossRef]
46. Rey, F.; Lopes, D.; Maciel, E.; Monteiro, J.; Skjermo, J.; Funderud, J.; Raposo, D.; Domingues, P.; Calado, R.; Domingues, M.R. Polar lipid profile of *Saccharina latissima*, a functional food from the sea. *Algal Res.* **2019**, *39*, 101473. [CrossRef]

47. Balboa, E.M.; Gallego-Fábrega, C.; Moure, A.; Domínguez, H. Study of the seasonal variation on proximate composition of oven-dried *Sargassum muticum* biomass collected in Vigo Ria, Spain. *J. Appl. Phycol.* **2016**, *28*, 1943–1953. [[CrossRef](#)]
48. Barbosa, M.; Fernandes, F.; Pereira, D.M.; Azevedo, I.C.; Sousa-Pinto, I.; Andrade, P.B.; Valentao, P. Fatty acid patterns of the kelps *Saccharina latissima*, *Saccorhiza polyschides* and *Laminaria ochroleuca*: Influence of changing environmental conditions. *Arab. J. Chem.* **2017**, *13*, 45–58. [[CrossRef](#)]
49. Fariman, G.A.; Shastan, S.J.; Zahedi, M.M. Seasonal variation of total lipid, fatty acids, fucoxanthin content, and antioxidant properties of two tropical brown algae (*Nizamuddinina zanardinii* and *Cystoseira indica*) from Iran. *J. Appl. Phycol.* **2016**, *28*, 1323–1331. [[CrossRef](#)]
50. Gosch, B.J.; Paul, N.A.; de Nys, R.; Magnusson, M. Spatial, seasonal, and within-plant variation in total fatty acid content and composition in the brown seaweeds *Dictyota bartayresii* and *Dictyopteria australis* (Dictyotales, Phaeophyceae). *J. Appl. Phycol.* **2015**, *27*, 1607–1622. [[CrossRef](#)]
51. Surget, G.; Le Lann, K.; Delebecq, G.; Kervarec, N.; Donval, A.; Poullaouec, M.A.; Bihannic, I.; Poupart, N.; Stiger-Pouvreau, V. Seasonal phenology and metabolomics of the introduced red macroalga *Gracilaria vermiculophylla*, monitored in the Bay of Brest (France). *J. Appl. Phycol.* **2017**, *29*, 2651–2666. [[CrossRef](#)]
52. Shannon, E.; Abu-Ghannam, N. Optimisation of fucoxanthin extraction from Irish seaweeds by response surface methodology. *J. Appl. Phycol.* **2017**, *29*, 1027–1036. [[CrossRef](#)]
53. Browse, J.; Warwick, N.; Somerville, C.R.; Slack, C.R. Fluxes through the prokaryotic and eukaryotic pathways of lipid synthesis in the '16:3' plant *Arabidopsis thaliana*. *Biochem. J.* **1986**, *235*, 25–31. [[CrossRef](#)]